SCIENTIFIC Publishing Limited

New Energy Exploitation and Application

http://ojs.ukscip.com/index.php/neea

Article

The Influence of Gas Pulsed Flow on Hydrodynamic Behaviors of Refined Standard Sugar

Trung Thanh Bui [1], Anh Duc Le [2,*] and Quang Phu Pham [1]

[1] Faculty of Heat & Refrigeration Engineering, Industrial University of Ho Chi Minh City, Ho Chi Minh City 727010, Vietnam

[2] Faculty of Engineering and Technology, Nong Lam University, Ho Chi Minh City 721400, Vietnam

[*] Correspondence: leanhduc@hcmuaf.edu.vn

Received: 5 May 2024; **Revised**: 13 June 2024;**Accepted**: 8 July 2024; **Published**: 15 July 2024

Abstract: The influence of gas-pulsed flow when supplied in the perpendicular direction to the refined standard (RS) sugar layer has been studied in this article. Some hydrodynamic parameters of the RS sugar in the gas-pulsed fluidized bed have also been determined. The research results have been applied in the design of the RS sugar dryer using the modern pulsed fluidized bed drying method. The bed porosity in the static particle layer (ε_0) was 0.44 while the bed porosity in the minimum fluidized bed (ε_{mg}) was 0.484 and the minimum fluidized bed velocity (U_{mg}) was 0.65 m/s. The bed porosity in the homogeneous fluidization bed (ε_{hg}) was 0.67, and the homogeneous fluidization velocity (U_{hg}) of 1.63 m/s has been calculated. The critical velocity (U_{cg}) of 2.7 m/s and the bed porosity (ε_{cg}) of 0.8 in the circulating particle bed were determined. The pressure drop through the layer of RS sugar with a thickness of 300 mm was 3808 N/m^2.

Keywords: hydrodynamics behaviors; bed porosity; refined standard sugar; minimum fluidized velocity; pressure drop

1. Introduction

Pulsed fluidized bed drying (PFBD) technology is categorized among the contemporary drying methods and equipment. The PFBD is presently undergoing extensive research and development by global scientists. This is largely due to its remarkable energy-saving capabilities during the drying of items in various sectors, such as food processing lines, pharmaceutical raw materials and chemical production [1].

This paper study the fluidization mechanisms and phenomena of dispersed and adhesive particles such as refined standard (RS) sugar using the batch gas pulsed fluidized bed dryer. Additionally, the article elucidates the methodology for evaluating fundamental hydrodynamic behaviors of RS sugar within a model of a batch PFB dryer, with a batch yield of 5 kg.

Refined standard (RS) sugar is a substance derived from the crystallization process. Following centrifugation, its moisture content typically ranges from 0.5% to 1.5% [2]. Immediate drying is imperative to prevent clumping, particularly under heat exposure, which exacerbates its tendency to adhere. This inherent adhesive quality poses challenges for continuous fluidized bed drying, further necessitating a meticulous approach to ensure the attainment of a superior-quality dried product [3].

Within the realm of pulsed fluidized bed methodologies, the gas inlet flow undergoes temporal alterations, consequently inducing shifts in the gas velocity during the bed's fluidization phase. This, in turn, prompts variations in the nature of the bubbling fluidized bed, exerting an impact on bed stability and

influencing the hydrodynamic characteristics within the fluidized state [4]. The use of pulsed gas flow has helped increase the mixing and turbulence between particles by up to 40% according to Pence and Beasley [5].

2. Data and Methods

2.1. The Formation of Fluidized Bed in Particle Layers

When a gas stream ascends through a layer of bulk solid particles, under conditions of low velocity and pressure, the particle layer remains stationary, which is referred to as the fixed bed state (depicted by the OA line in Figure 1 and Figure 2a). The velocity of the gas is represented as U_s. With a gradual increase in gas velocity, the bulk of solid particles begins to expand, causing a rise in bulk volume. Adjacent particles progressively separate as a balance emerges between the frictional force among particles and the force exerted by the gas stream, counteracting particle gravity. This nullifies the vertical component of compressive force between neighboring particles. At this juncture, the layer of particles is termed the minimum fluidized bed, indicative of its liquid-like qualities, as illustrated in Figure 2b. The gas stream's velocity through the particle layer is now termed the minimum fluidization velocity, denoted as U_{mg}.

This pivotal juncture is marked as point A in Figure 1.

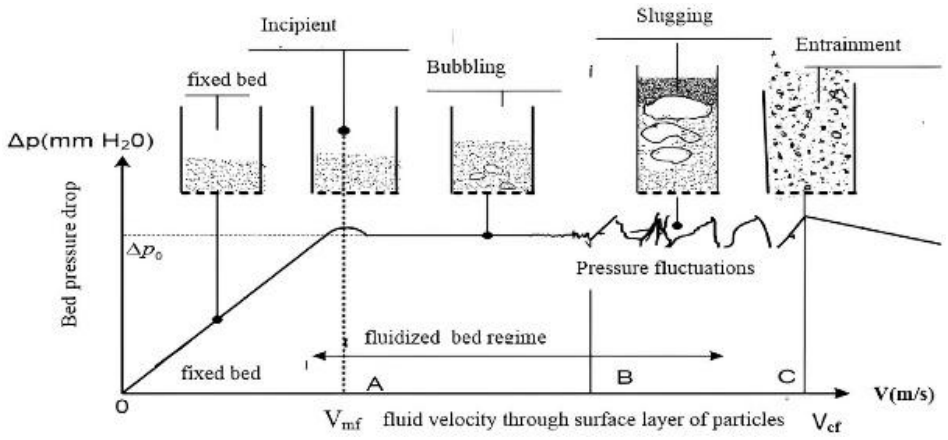

Figure 1. Graph showing the states of bed in continuous fluidized bed drying [6].

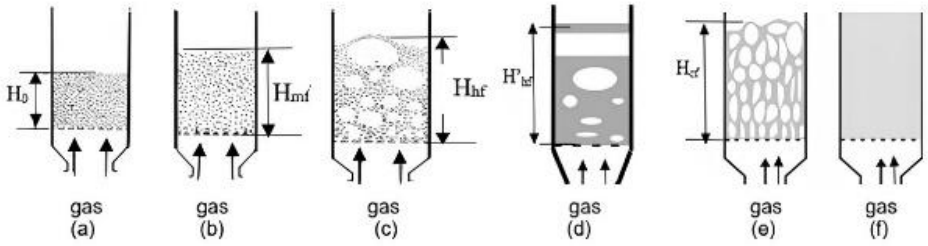

Figure 2. The fluidized bed states with changes in the gas velocity through the bed [7]. (**a**) fixed bed; (**b**) minimum fluidized bed; (**c**) bubbling fluidized bed; (**d**) axial slugging bed; (**e**) turbulent fluidized bed; (**f**) pneumatic transportation.

By elevating the velocity of the hot gas stream to a point where uniform and vigorous fluidization of the entire array of dried particles is achieved, the gas velocity is now denoted as U_{hf}. In this scenario, the upward pull of the gas stream precisely counterbalances the downward force of gravity on the particles, thereby suspending them within the gas flow. This results in a cohesive and uniformly fluidized layer of dried particles—an instance of a homogeneous fluidization bed. The stabilized state of the bed is exemplified in Figure 2c. The specific gas velocity at this juncture is determined by the interval A–B in Figure 1. Notably, the particle layer exhibits a

diverse dispersion of sizes and masses. Consequently, particles possessing a lower density than the bulk will float atop the bed, while those with greater density will sink to its base. As a result, the bed experiences a perpetual rise and fall-phenomenon [6].

As the gas velocity continues to rise, the particles in the bulk also undergo increased expansion. Consequently, the bulk density experiences a consistent decline. This progression leads to a pronounced occurrence of fluidization, causing substantial separation among the particles. Upon surpassing a critical gas velocity within the bed, the inter-particle bonding at the upper layer of the bed weakens. As a result, particles initiate detachment from the bed surface and become entrained by the fluidic motion, ultimately exiting the drying chamber. This specific state of the bed is depicted in Figure 2f.

Referring to this stage, the velocity of the drying agent is denoted as U_{cg}. Notably, during this phase, the resistance encountered by the gas stream as it passes through the bed diminishes, with the pressure drop across the bed now designated as ΔP_C, indicating that it is less than ΔP_A as illustrated in Figure 1. In the moments just before a particle is entirely carried away, the pressure loss across the bed becomes unstable, characterized by a cyclic fluctuation involving alternating increases and decreases [6].

As previously stated, the inherent variability in the sizes of dried particles—both in their natural state and as influenced by processing technology—becomes apparent. This becomes particularly evident when elevating the gas velocity through the bed beyond the minimum fluidization threshold (illustrated by the transition from point A to B to C in Figure 1). Consequently, various types of fluidized beds manifest, encompassing the following categories: (i) bubbling bed, as depicted in Figure 2c; (ii) channeling bed, as shown in Figure 2d; (iii) axial slugging bed, represented by Figure 2e; (iv) entrainment bed, visualized in Figure 2f.

The disruption of the fluidized bed, often referred to as the pseudo-liquid layer, is evident in the fluidization curve graph. This curve is constructed based on the correlated connection between the gas pressure across the bed and the gas velocity across the fluidized bed's surface. This phenomenon is illustrated in Figure 1 for continuous fluidized bed drying [6], as well as in Figure 3 for batch pulsed fluidized bed drying [7].

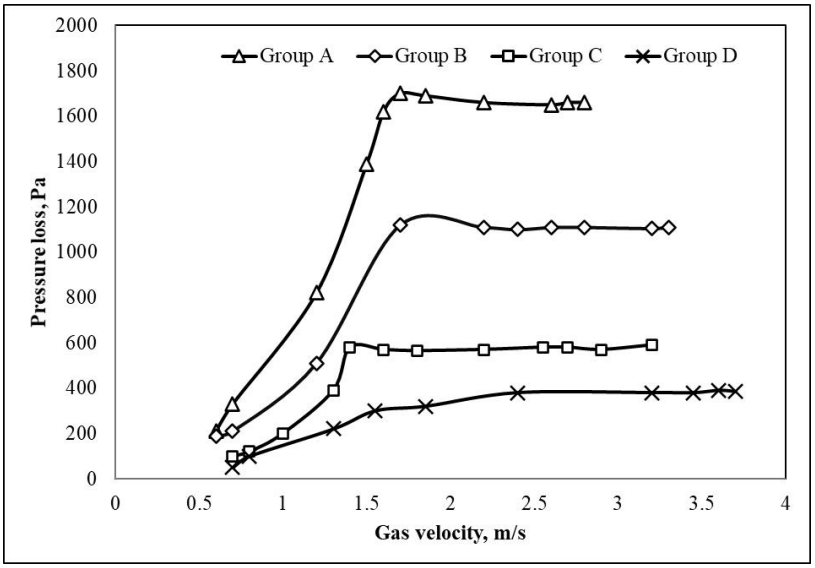

Figure 3. The fluidization curve through a bed of pulsed-type rotating disk with different particles (frequency of 6.28/s, A: 222 kg/m^2; B: 159 kg/m^2; C: 96 kg/m^2; D: 64 kg/m^2) [7,8].

2.2. Basic Hydrodynamics Behaviors of Fluidized Bed

2.2.1. Gas Velocity and Minimum Fluidization Pressure Drop

Irrespective of the circumstances, when introducing a gas flow rate (Q_g) to the particle layer from below in a direction perpendicular to the gas distributor, the superficial velocity (i.e., the gas velocity across the particle layer's surface) is established through the use of Equation (1):

$$U_g = \frac{Q_g}{A} \tag{1}$$

When the bed of particles begins to fluidize, this value of gas velocity is determined by Equation (2):

$$U_{mg} = \frac{Q_{mg}}{A} \tag{2}$$

According to reference [6], when dealing with spherical particles having a diameter d_p ≤ 0.1 mm and operating within the constraints of a Reynolds number (Re ≤ 10) for gas flow calculations, Equation (3) comes into play. This particular equation, as introduced by Kozeny-Carman [6], finds its utility in scenarios where gas streams are analyzed while factoring in the dynamic viscosity.

$$U_{mg} = \frac{(\rho_p - \rho_f) g d_p^2 \varepsilon_{mg}^3}{150 \mu_g (1 - \varepsilon_{mg})} \tag{3}$$

As outlined by McCabe, Smith, and Harriott [9], the range of (ε_{mg}) for spherical particles in a minimum fluidized state spans from 0.4 to 0.45. Nonetheless, in the case of particles classified as type D [10] and featuring a diameter (d_p) greater than 1mm – particles that experience the influence of inertial forces during fluidization—the gas velocity for achieving minimum fluidization must be derived through the utilization of Equation (4), known as the Ergun equation [11]:

$$\frac{\Delta P}{H_{mg}} = \frac{150 \mu_g (1 - \varepsilon_{mg})^2 U_{mg}}{\varepsilon_{mg}^3 d_p^2} + \frac{1.75 (1 - \varepsilon_{mg}) \rho_g U_{mg}^2}{\varepsilon_{mg}^3 d_p} \tag{4}$$

For particles with arbitrary shapes and size distributions, Equation (5) is used:

$$\frac{\Delta P}{H_{mg}} = 150 \frac{\left(1 - \varepsilon_{mg}\right)^2}{\varepsilon_{mg}^3} \frac{\mu_g U_{mg}}{\left(\phi d_m\right)^2} + 1.75 \frac{\left(1 - \varepsilon_{mg}\right)}{\varepsilon_{mg}^3} \frac{\rho_g U_{mg}^2}{\phi d_m} \tag{5}$$

By considering Equations (4) and (5), it becomes apparent that the pressure drop across the fluidized bed is contingent upon several factors, including particle diameter, the height of the fluidized bed, dynamic viscosity, and the density of the gas introduced into the drying bed. At the minimum fluidization state, the volume of the particle bed (U_{mg}) can be calculated using Equation (6):

$$U_{mg} = (1 - \varepsilon_{mg}) A H_{mg} \tag{6}$$

The gravitational weight (W) of the particle bed at this state is calculated using Equation (7):

$$W = (1 - \varepsilon_{mg})(\rho_p - \rho_g) A H_{mg} g \tag{7}$$

In theory, for particles to be fluidized, the actual weight of the particle bed must be balanced by the force exerted upwards by the gas, represented by the pressure drop across the bed (ΔP) multiplied by the area of the gas distribution grid (A). The balance equation for the real weight of the particle bed and the upward force of the gas can be established as Equation (8) [6]:

$$\Delta P = (1 - \varepsilon_{mg})(\rho_p - \rho_g) H_{mg} g \tag{8}$$

Combining Equations (4), (5), and (8), the gas velocity (U_{mg}) through the particle bed with any shape (not just spherical) is determined as follows, Equation (9):

$$g(\rho_p - \rho_g) = 150 \frac{\left(1 - \varepsilon_{mg}\right)}{\varepsilon_{mg}^3} \frac{\mu_g U_{mg}}{\left(\phi d_m\right)^2} + 1.75 \frac{\rho_g U_{mg}^2}{\varepsilon_{mg}^3 \left(\phi d_m\right)} \tag{9}$$

And the pressure drop across the fluidized bed is calculated as Equation (10) [6]:

$$\Delta P = m(\rho_p S_{ps})(\rho_p - \rho_g) g \tag{10}$$

Furthermore, according to reference [6], the pressure loss across the fluidized bed can also be calculated using Equation (11):

$$\Delta P = \frac{m}{\rho_p A}(\rho_p - \rho_g)g \tag{11}$$

In addition, according to reference [11], the pressure loss through the homogeneous fluidized bed can be calculated by Equation (12):

$$\Delta P = g\rho_p\left(1-\frac{\rho_g}{\rho_p}\right)H_{mg} \tag{12}$$

According to McCabe, Smith, and Harriott [9], the gas velocity U_{mg} can be calculated using Equation (9) based on an assumed porosity ε_{mg} = 0.5. However, according to Lewis Orchard [9], for particles with arbitrary shapes, the gas velocity U_{mg} is determined by Equation (13):

$$U_{mg} \approx \frac{g(\rho_p - \rho_g)}{150\mu_g}\frac{\varepsilon_{mg}^{\ 3}}{1-\varepsilon_{mg}}\phi^2 d_m^2 \tag{13}$$

2.2.2. Gas Velocity in Bubbling Fluidized Bed

With the augmentation of gas velocity (U_g) traversing the bed surface, surpassing the minimum fluidization velocity (U_{mg}), a phenomenon unfolds where gas bubbles materialize and ascend through the particle-laden bed. At the onset, minute gas bubbles materialize at the gas distribution plate, subsequently amalgamating and expanding as they journey through the bed. This bubble formation contributes to an expansion of the bed's volume. In the context of bubbling fluidization, a notable aspect is the absence of a temperature gradient within the fluidized particle range [12]. In this scenario, the bed attains an isothermal equilibrium state.

If we define f_b as the volume fraction of space occupied by the gas bubbles, the volume balance equation for the gas stream through the drying bed can be established as Equation (14):

$$U_b = f_b u_b + (1-f_b)U_{hg} \tag{14}$$

The term $f_b \times u_b$ represents the gas stream rate per area through the bubble phase, while (1 - f_b). U_{hg} represents the gas stream rate per area through the fluidizing phase.

Based on this, a volume balance equation for the particle phase can be established, Equation (15):

$$H_{hg} = H_0(1-f_b) \tag{15}$$

Due to the participation of the gas bubble volume fraction (f_b) in the fluidized bed, we can establish Equation (16):

$$\frac{H_{hg}}{H_{mg}} = \frac{u_b - U_{mg}}{u_b - U_{hg}} \tag{16}$$

According to reference [13], an experimental formula for calculating the gas bubble velocity, given by Equation (17):

$$u_b = 0.71\sqrt{gD_b}\ \text{m/s} \tag{17}$$

Davidson and Harrison [6] proposed an empirical formula for the gas bubble velocity, Equation (18):

$$u_b = 0.35\sqrt{gD_c} \tag{18}$$

2.2.3. Critical Gas Velocity Through the Bed

As detailed in reference [6], the gas velocity's progression through the bed extends beyond the point of bubbling velocity. Once it reaches a sufficiently elevated level capable of lifting and transporting particles out of the bed, it's identified as the critical gas velocity (U_{cg}). The depiction in Figure 1 [6] delineates the fluidization behavior of the particle bed, contingent upon the gas velocity. Point C on this graph signifies the critical velocity. In the context of both general fluidized bed drying and fluidized bed combustion, it's imperative to ensure that

the gas velocity (U_g) directed through the bed maintains the fluidized bed condition ($U_g < U_{cg}$) to prevent particle entrainment from the bed.

For particles with arbitrary shapes and non-uniform size distributions, the Reynolds number (Re) is calculated based on the mean particle diameter (d_m) and the sphericity (ϕ) by Equation (19) [6].

$$\mathrm{Re} = \frac{\rho_g U_g \phi d_m}{\mu_g} \tag{19}$$

According to reference [6], at position B (Figure 1), the critical gas velocity for the bed with arbitrary shape in a laminar flow regime (Re < 1) is calculated by Equation (20) [13].

$$U_{cg} = \frac{g(\rho_p - \rho_g)}{18\mu_g} \frac{1}{1-\varepsilon_{cg}} \phi d_m^2 \tag{20}$$

For the transitional flow regime (1 < Re < 500), the critical gas velocity is given by Equation (21) [13].

$$U_{cg} = \left[\frac{4(\rho_p - \rho_g)g}{3\rho_g C_D} \phi d_m\right]^{1/2} \tag{21}$$

where C_D is the drag coefficient: $C_D = \frac{18}{\mathrm{Re}^{3/5}}$.

In the turbulent flow regime (500 < Re < 200,000), the critical gas velocity is determined as Equation (22) [13].

$$U_{cg} = \left[\frac{3(\rho_p - \rho_g)g}{\rho_g} \phi d_m\right]^{1/2} \tag{22}$$

2.2.4. Porosity of the Particle Bed

Porosity, commonly referred to as bed voidage, stands as a vital parameter in the realm of hydrodynamic calculations within the context of batch fluidized bed dryer for RS sugar. The determination of porosity for RS sugar within the fixed bed is accomplished through the utilization of Equation (23) [6].

$$\varepsilon_0 = \left(1 - \frac{\rho_b}{\rho_p}\right) \tag{23}$$

The bed porosity at the minimum fluidization state can be calculated experimentally using the empirical formula, Equation (24) [14]:

$$\varepsilon_{mg} = k\varepsilon_0 \tag{24}$$

where k is a coefficient within the range of 1.1–1.2.

In the homogeneous fluidization bed, the bed porosity can be calculated using Equation (25) [6]:

$$\varepsilon_{hg} = \left(\frac{18\,\mathrm{Re}_{hg} + 0{,}36\,\mathrm{Re}_{hg}^2}{Ar}\right)^{0.21} \tag{25}$$

3. Results and Discussion

With the objective of enhancing the quality of RS sugar within sugar mills through the drying procedure, an empirical investigation involving the utilization of a pulsed fluidized bed dryer, possessing a 5 kg/batch capacity, was undertaken. The particulars concerning RS particle attributes were previously documented, encompassing the mean diameter (d_m = 0.892 mm) and sphericity (ϕ = 0.85) [15]. Thus, the particle's equivalent diameter was determined as $d_p = \phi \times d_m$ = 0.76 mm, assuming a spherical morphology. The fixed bed's bulk density for RS sugar, exhibiting a moisture content of 1.5–2%, was ρ_b = 889 kg/m^3, while the particle density at ρ_p = 1598 kg/m^3.

The drying medium, derived from the ambient air at an average temperature of 28 °C and relative humidity of 80%, underwent heating to reach t_g = 70 °C. The air possessed a density of ρ_g = 1.045 kg/m^3 and a dynamic viscosity of $\mu_g = 20.35\mathrm{e}-6$ N·s/m^2. The static bed layer's thickness atop the distribution plate was denoted as

H_0 = 0.3 m. In line with these parameters, the investigation pursued the drying of RS using the aforementioned pulsed fluidized bed dryer setup.

Our team of researchers conducted thorough calculations aimed at elucidating the hydrodynamic characteristics of the RS sugar bed across distinct phases, encompassing static, minimum fluidization, homogeneous fluidization, and critical fluidization states. This comprehensive analysis led to the derivation of the subsequent outcomes.

3.1. Minimum Fluidization State

The void fraction of the RS sugar bed in the fixed bed according to the Equation (23) [6] is determined by Equation (26):

$$\varepsilon_0 = \left(1-\frac{\rho_b}{\rho_p}\right) = \left(1-\frac{889}{1598}\right) = 0.44 \tag{26}$$

The porosity of the bed in the minimum fluidization is calculated using the Equation (24) [14]: $\varepsilon_{mg} = \varepsilon_0 \times 1.1 = 0.484$.

From Equation (13) [6], the minimum fluidization velocity is determined by Equation (27):

$$U_{mg} = \frac{(1598-1.045)\times 9.81\times(760\times10^{-6})^2\times 0.484^3}{150\times 20.35\times10^{-6}\times(1-0.484)} = 0.65\,\text{m/s} \tag{27}$$

3.2. Homogeneous Fluidization State

According to references [14,16], the air velocity through the distributor to fluidize the RS sugar is reasonably calculated using Equation (28):

$$U_{hg} = (2\div 3)U_{mg} \tag{28}$$

So the reasonable fluidization velocity value is determined: U_{hg} = 2.5 × U_{mg} = 1.63 m/s.

The Reynolds number in the homogeneous fluidization state, determined using Equation (19), is Re = Re_{hg} with U_{hg} = 1.63 m/s [6] as described in Equation (29):

$$\text{Re}_{hg} = \frac{\rho_g U_g \phi d_m}{\mu_g} = \frac{1.045\times1.63\times760\times10^{-6}}{20.35\times10^{-6}} = 63.6 \tag{29}$$

The bed porosity in the homogeneous fluidization state is calculated using Equation (25) [6] and the result is presented in Equation (30).

$$\begin{aligned}\varepsilon_{hg} &= \left(\frac{18\,\text{Re}_{hg}+0.36\,\text{Re}_{hg}^2}{Ar}\right)^{0.21} \\ &= \left(\frac{18\times63.6+0.36\times63.6^2}{17353.6}\right)^{0.21} = 0.67\end{aligned} \tag{30}$$

3.3. Critical Fluidization State

The condition of critical fluidization [13] (signifying the instability of the fluidized bed) indicates that particles are poised to be entrained by the drying agent. This critical state is illustrated at the B–C position in Figure 1 [6], where the bed remains inherently unsettled and is readily carried out of the drying chamber when the gas velocity surpasses the critical velocity (U_{cg}) [13].

In order to establish a foundation for defining an appropriate size for the gas separation chamber in the PFB (Pulsed Fluidized Bed) dryer, we ascertain the theoretical critical velocity as the fundamental metric for evaluating the cross-sectional area of the particle separation chamber, prior to the exit of the moist gas.

According to reference [6], the Archimedes number (Ar) is calculated for particles of any shape (spherical particles) [6] by Equation (31):

$$Ar = \frac{\rho_g(\rho_p - \rho_g)g(\phi d_m)^3}{\mu_g^2} \tag{31}$$

Hence, the outcome of the Archimedes number is obtained by Equation (32) [6].

$$Ar = \frac{9.81\times\left(760\times10^{-6}\right)^3\times1.045\times(1598-1.045)}{(20.35\times10^{-6})^2} = 17353.6 \tag{32}$$

On the other hand, by transformations from Ergun's equation for any particle with spherical calculation ϕ, the relationship equation between the Ar and Re numbers along with the porosity of the fluidized bed was established by Equation (33) [6,11].

$$Ar = 150\frac{(1-\varepsilon_{hg})}{\phi^2\,\varepsilon_{hg}^3}\mathrm{Re}_{hg} + \frac{1.75}{\phi\varepsilon_{hg}^3}\mathrm{Re}_{hg}^2 \tag{33}$$

Substituting the values of ε_{hg} = 0.484, the sphericity for sugar particles ϕ = 0.85 into Equation (33) and Equation (33) becomes a quadratic equation [6], as described in Equation (34):

$$6.85\,\mathrm{Re}_{hg}^2 + 227.79\,\mathrm{Re}_{hg} - 17353.6 = 0 \tag{34}$$

Solving the above equation, get the only solution Re_{hg} = 36.4, and remove the solution Re_{hg} = -69.6 because only positive values were taken.

From the results of Re_{hg}, with the minimum fluidization state Re_{hg} = 36.4, the gas streams through the bed were in the transition mode (1< Re < 500).

According to Equation (21), the critical velocity (U_{cg}) was determined by Equation (35) [13]:

$$\begin{aligned} U_{cg} &= \left[\frac{4(\rho_p-\rho_g)g}{3\rho_g C_D}\phi d_m\right]^{1/2} \\ &= \left[\frac{4(1598-1.045)\times9.81}{3\times1.045\times2.1}(0.85\times892\times10^{-6})\right]^{1/2} = 2.7\,\mathrm{m/s} \end{aligned} \tag{35}$$

where the resistance coefficient C_D had the value: $C_D = \frac{18}{Re^{3/5}} = \frac{18}{36.4^{3/5}} = 2.1$.

Throughout the practical drying process, in order to guarantee both drying efficiency and product quality, the operator of the dryer must fine-tune the fan's airflow and the frequency of air delivery into the drying chamber to achieve an optimal velocity. This optimal velocity (U_g) should fall within the range defined by $U_{mg} < U_{hg} < U_{cg}$.

For the computation of bed porosity within the critical fluidization state, corresponding to the critical gas velocity (U_{cg}), the utilization of Equation (19) yields the porosity value. By substituting the specific value (U_{cg} = 2.7 m/s) into the equation, the Re_{cg} value is redefined by Equation (36) [6]:

$$\mathrm{Re}_{cg} = \frac{\rho_g U_g \phi d_m}{\mu_g} = \frac{1.045\times2.7\times760\times10^{-6}}{20.35\times10^{-6}} = 105.4 \tag{36}$$

Substituting Re_{cg} = 105.4 in Equation (25), the bed porosity in the critical fluidization state (ε_{cg}) was found in Equation (37) [6].

$$\begin{aligned} \varepsilon_{cg} &= \left(\frac{18\,\mathrm{Re}_{cg} + 0.36\,\mathrm{Re}_{cg}^2}{Ar}\right)^{0.21} \\ &= \left(\frac{18\times105.4 + 0.36\times105.4^2}{17353.6}\right)^{0.21} = 0.8 \end{aligned} \tag{37}$$

The porosity of the particle bulk becomes ε = 1 when the bed transitions into the pneumatic transportation state.

3.4. Calculation of the Pressure Loss of the Gas Stream Through the Pulsed Fluidized Bed

Pressure drop through the fixed bed or fluidized bed stands as a critical factor in the computation for designing a PFB dryer. The pressure drop across the fixed bed at position A (refer to Figure 1) is determined utilizing the Ergun equation [11], represented as Equation (38).

Leveraging the acquired numerical values, the pressure loss across the RS sugar bed is subsequently evaluated.

The resistance encountered through the fixed bed at position A (as indicated in Figure 1) in the RS sugar dryer encompasses the aforementioned input parameters, with the static height H_0 maintained at 300 mm. According to Ergun equation [11]:

$$\frac{\Delta P}{H} = \frac{150\mu_g(1-\varepsilon_{mg})^2 U_{mg}}{\varepsilon_{mg}^{\ 3}(\phi d_m)^2} + \frac{1.75(1-\varepsilon_{mg})\rho_g U_{mg}^{\ 2}}{\varepsilon_{mg}^{\ 3}\phi d_m} \tag{38}$$

Substituting the obtained values into Equation (38), the pressure loss through the RS sugar bed was calculated by Equation (39) [6,11].

$$\Delta P = 0.3\left[\begin{array}{l}\dfrac{150\times 20.35\times 10^{-6}(1-0.484)^2\times 0.65}{0.484^3\left(760\times 10^{-6}\right)^2} \\ +\dfrac{1.75\times(1-0.484)\times 1.045\times 0.65^2}{0.484^3\times 760\times 10^{-6})}\end{array}\right] = 3808\ \mathrm{N/m^2} \tag{39}$$

4. Conclusions

Building upon the groundwork laid by prior researchers, this study delved into the fluidization behaviors integral to pulsed fluidized bed drying technology applied to RS sugar. The investigation systematically unveiled the intricacies of fluidization phenomena across distinct particle bed states and diverse fluidized particle bed configurations, all orchestrated by varying gas velocities.

In terms of practical implications, this research supplied invaluable insights into the RS sugar drying process via the utilization of a pulsed fluidized bed dryer. Particularly noteworthy were the determinations of porosity in various bed states: ε_0 = 0.44 for the fixed bed, ε_{mg} = 0.484 for the minimum fluidized bed, ε_{hg} = 0.67 for the homogeneous fluidized bed, and ε_{cg} = 0.8 for the critical bed. Moreover, the study accurately pinpointed essential thresholds such as the minimum fluidization velocity (U_{mg} = 0.65 m/s), homogeneous fluidization velocity (U_{hg} = 1.63 m/s), and critical velocity (U_{cg} = 2.7 m/s).

Furthermore, the investigation yielded a computed pressure loss of 3808 N/m^2 across the RS sugar bed, configured with a thickness of H = 300 mm. These revelations collectively contributed to refining the optimization of sugar drying processes, ultimately elevating the quality of the end sugar product.

Nomenclature

A	area of the gas distributor, m^2;
D_b	diameter of the gas bubbles, taken as the diameter of a sphere with the same bubble volume;
D_c	diameter of gas distributor (the drying chamber and the gas distributor are circular in shape);
d_m	mean diameter of the particles, m;
d_p	diameter of spherical particles, m;
f_b	volume fraction of gas bubbles, m^3;
g	gravity acceleration, m/s^2;
H_0	height of the fixed bed, m;
H_{hg}	height of homogeneous fluidization bed, m;
H_{mg}	the bed height in minimum fluidization state, m;
Q_g	gas flow rate, m^3/s;
Q_{mg}	gas flow rate in minimum fluidization state, m^3/s;
S_{ps}	area of the drying bed, m^2;
u_b	average velocity of the gas bubbles, m/s;
U_g	superficial velocity, m/s;

U_{hg}	gas velocity through the homogeneous fluidization bed, m/s;
U_{mg}	minimum fluidization velocity, m/s;
ϕ	sphericity of particle;
ρ_b	bulk density, kg/m^3;
ε_{cg}	porosity of the bed at the critical velocity;
μ_g	dynamic viscosity of gas, Pa·s;
ρ_g	gas density, kg/m^3;
ε_{mg}	porosity in minimum fluidization state;
ρ_p	particle density, kg/m^3;
ΔP	pressure drop across the minimum fluidized bed, N/m^2.

Author Contributions

Introduction, T.T.B. and A.D.L.; Data and Methods, T.T.B.; analysis and calculation, Q.P.P.; writing – original draft preparation, T.T.B.; writing—review and editing, A.D.L.; supervision, T.T.B. and A.D.L. All authors have read and agreed to the published version of the manuscript.

Funding

This work received no external funding.

Institutional Review Board Statement

Not applicable.

Informed Consent Statement

Not applicable.

Data Availability Statement

Due to confidentiality, no data was available at this time.

Acknowledgments

The authors are grateful to the Faculty of Heat and Refrigeration Engineering, IUH for supporting equipment and apparatus to carry out this research.

Conflicts of Interest

The authors declare no conflict of interest.

References

1. Kudra, T.; Mujumdar. A.S. *Advanced Drying Technologies*, 2nd ed.; CRC Press: Boca Raton, FL, USA, 2009; 438p. [CrossRef]
2. Baikow, V.E. Raw Sugar. In *Manufacture and Refining of Raw Cane Sugar*, 2nd ed.; Baikow, V.E., Eds.; Elsevier: Amsterdam, Netherlands, 2013; pp. 240–254. [CrossRef]
3. Meadows, D. Somewhat Dry... A New Look at the Conditioning of Refined Sugar. In Proceedings of The South African Sugar Technologists' Association, Durban, South Africa, June 1993.
4. Coppens, M.O.; Van Ommen, J.R. Structuring Chaotic Fluidized Beds. *Chem. Eng. J.* **2003**, *96*, 117–124. [CrossRef]
5. Pence, D.V.; Beasley, D.E. Chaos Suppression in Gas-Solid Fluidization. *Chaos* **1998**, *8*, 514–519. [CrossRef]
6. Howard, J.R. *Fluidized Bed Technology, Principles and Applications*; Taylor & Francis Group: Bristol, UK, 1989; 214p.
7. Geldart, D. The Effect of Particle Size and Size Distribution on the Behaviour of Gas-Fluidised Beds. *Powder Technol.* **1972**, *6*, 201–215. [CrossRef]
8. Elenkov, V.R.; Djurkov, T.G. A fluidized bed with jet-pulsed agitation of fluidization. In Proceedings of the First South East European Symposium–Fluidized Bed in Energy Production, 2001, pp. 105–116.
9. McCabe, W.L.; Smith, J.C.; Harriott, P. *Scilab Code for Unit Operations of Chemical Engineering*, 5th ed.; McGraw-Hill: New Delhi, India, 1993; 175p.
10. Geldart, D. Types of Gas Fluidization. *Powder Technol.* **1973**, *7*, 285–292. [CrossRef]

11. Ergun, S. Fluid Flow Through Packed Columns. *Chem. Eng. Prog.* **1952**, *48*, 89–94.
12. Levenspiel, O. *Engineering Flow and Heat Exchange*, 1st ed.*;* Springer: New York, NY, USA, 1985; 366p. [CrossRef]
13. Kunii, D.; Levenspiel, O. High-Velocity Fluidization. In *Fluidization Engineering*, 2nd ed.; Kunii, D., Levenspiel, O., Eds.; Butterworth-Heinemann: Stoneham, MA, USA, 1991; pp. 193–210. [CrossRef]
14. Ginzburg, A.S. *Theoretical and Technical Basis of Drying Food Products*. Pishchevaya Promyshlennost: Moscow, Russian, 1973.
15. Pham, Q.P.; Bui, T.T.; Le, A.D. Determination on the Geometrical Parameters of a RS Sugar Cane Particle to Design a the Pulsed Fluidized Bed Dryer. *Sci. Technol. J.* **2022**, *20*, 44–57. (in Vietnamese).
16. Tran Van Phu. *Drying Technology.* Educational Publishing House, 2008, pp 267. ISBN: 200288. (in Vietnamese).